Hemoprotein Bioconjugates of Gold and Silver Nanoparticles and Gold Nanorods: Structure−Function Correlations

Renjis T. Tom, A. K. Samal, T. S. Sreeprasad, and T. Pradeep*

DST Unit on Nanoscience, Department of Chemistry and Sophisticated Analytical Instrument Facility, Indian Institute of Technology Madras, Chennai - 600 036, India

Received April 28, 2006. In Final Form: October 27, 2006

Bioconjugates of the hemoproteins, myoglobin, and hemoglobin have been synthesized by their adsorption on spherical gold and silver nanoparticles and gold nanorods. The adsorption of hemoproteins on the nanoparticle surface was confirmed by their molecular ion signatures in matrix assisted laser desorption ionization mass spectrometry and specific Raman features of the prosthetic heme *b* units. High-resolution transmission electron microscopy (HRTEM) and UV−visible spectroscopy showed that the particles retain their morphology and show aggregation only in the case of silver. The binding of azide ion to the Fe(III) center of the prosthetic heme *b* moiety caused a red shift of the Soret band, both in the case of the bioconjugates and in free hemoproteins. This was further confirmed by the characteristic signature at 2050 cm^{-1} in the Fourier-transform infrared spectra, which corresponds to the asymmetric stretching of the Fe(III) bound azide. The retention of the chemical behavior of the prosthetic heme group after adsorption on the nanoparticle is interesting due to its implications in nanoparticle supported enzyme catalysis. The absence of morphology changes after the reaction of bioconjugates with azide ion observed in HRTEM studies implies the stability of nanoparticles under the reaction conditions. All these studies indicate the retention of protein structure after adsorption on the nanoparticle surface.

Introduction

The chemistry of biological macromolecules like proteins and nucleic acids is different from other molecules, due to the high specificity and selectivity of the processes involved. This arises from the confined nature of the microenvironment around the reaction center. Spectroscopic investigations of the chemistry occurring in the biological systems are difficult due to the low concentration of the analyte molecules, often below the detection limit, and interference of other molecules in the spectroscopic range. One can overcome these drawbacks by the immobilization of the molecule of interest on nanoparticle surfaces.[1,2] Noble metal nanoparticles are unique supports to study the chemistry of biomolecules because of the size compatibility, chemical inertness, and high dispersibility in the aqueous medium.[3,4] The metal nanoparticle−protein conjugates have been applied as electron dense biospecific stains for transmission electron microscopy of biological specimens because of the retention of biological activity of the proteins after immobilization on the nanoparticle surface.[5] The intense and sensitive optical absorption band of the nanoparticles strengthens their utility as probes for several biomolecular processes and targeted cellular imaging.[6] Polynucleotide detection using gold nanoparticle bioconjugates was used in an approach that utilized the alteration in optical properties ensuing from plasmon−plasmon coupling between adjacent gold nanoparticles.[7] Incident light impinging nanoparticle surfaces excites conduction band electrons and stimulates the excitation of surface plasmons effecting huge electromagnetic enhancement of Raman[8,9] and fluorescence[10,11] spectral features, and these phenomena are used for the ultrasensitive detection of biomolecules. Plasmon resonant silver nanoparticles capped with target-specific biomolecules showed better performance for in situ DNA hybridization[12] and immunocytology assay,[13] compared to the conventional methodologies based on radioactivity, fluorescence, chemiluminescence, or colorimetry. Surface enhancement of Raman vibrations of prosthetic heme *b* moiety of hemoglobin (Hb)[14] and myoglobin (Mb)[15] immobilized on silver nanoparticles was utilized for single molecule spectroscopy. The surface immobilization of biomolecules on nanoparticles was also utilized in protein analysis using matrix assisted laser desorption ionization time-of-flight mass spectrometry (MALDI-TOF MS).[16,17] Encapsulation of gold-cytochrome *c* (Cyt. *c*) bioconjugates in porous silica superstructures lead to an aerogel which was used for sensing NO.[18,19] The biological activity of

* To whom correspondence should be addressed. E-mail: pradeep@iitm.ac.in. Fax: 044-2257 0545/0509.

(1) Gole, A.; Dash, C.; Ramakrishnan, V.; Sainkar, S. R.; Mandale, A. B.; Rao, M.; Sastry, M. *Langmuir* **2001**, *17*, 1674−1679.
(2) Stuart, D. A.; Haes, A. J.; Yonzon, C. R.; Hicks, E. M.; Duyne, R. P. V. *IEE Proc.-Nanobiotechnol.* **2005**, *152*, 13−32.
(3) Mirkin, C. A.; Letsinger, R. L.; Mucic, R. C.; Storhoff, J. J. *Nature* **1996**, *382*, 607−609.
(4) Alivisatos, A. P.; Johnsson, K. P.; Peng, X.; Wilson, T. E.; Loweth, C. J.; Bruchez, M. P., Jr.; Schultz, P. G. *Nature* **1996**, *382*, 609−611.
(5) Hayat, M. A., Ed. *Colloidal Gold: Principles, Methods and Applications*; Academic Press: New York, 1989 (in three volumes).
(6) Sokolov, K.; Follen, M.; Aaron, J.; Pavlova, I.; Malpica, A.; Lotan, R.; Richards-Kortum, R. *Cancer Res.* **2003**, *63*, 1999−2004.
(7) Elghanian, R.; Storhoff, J. J.; Mucic, R. C.; Letsinger, R. L.; Mirkin, C. A. *Science* **1997**, *277*, 1078−1081.
(8) Keating, C. D.; Kovaleski, K. M.; Natan. M. J. *J. Phys. Chem. B* **1998**, *102*, 9404−9413.
(9) Keating, C. D.; Kovaleski, K. M.; Natan. M. J. *J. Phys. Chem. B* **1998**, *102*, 9414−9425.
(10) Aslan, K.; Leonenko, Z.; Lakowicz, J. R.; Geddes, C. D. *J. Phys. Chem. B* **2005**, *109*, 3157−3162.
(11) Aslan, K.; Lakowicz, J. R.; Geddes, C. D. *J. Phys. Chem. B* **2005**, *109*, 6247−6251.
(12) Oldenburg, S. J.; Genick, C. C.; Clark, K. A.; Schultz, D. A. *Anal. Biochem.* **2002**, *309*, 109−116.
(13) Schultz, S.; Smith, D. R.; Mock, J. J.; Schultz, D. A. *Proc. Natl. Acad. Sci. U.S.A.* **2000**, *97*, 996−1001.
(14) Xu, H.; Bjerneld, E. J.; Käll, M.; Börjesson, L. *Phys. Rev. Lett.* **1999**, *83*, 4357−4360.
(15) Bizzarri, A. R.; Cannistraro, S. *Appl. Spectrosc.* **2002**, *56*, 1531−1537.
(16) Teng, C. H.; Ho, K. C.; Lin, Y. S.; Chen, Y. C. *Anal. Chem.* **2004**, *76*, 4337−4342.
(17) Ho, K. C.; Tsai, P. J.; Lin, Y. S.; Chen, Y. C. *Anal. Chem.* **2004**, *76*, 7162−7168.
(18) Wallace, J. M.; Rice, J. K.; Pietron, J. J.; Stroud, R. M.; Long, J. W.; Rolison, D. R. *Nano Lett.* **2003**, *3*, 1463−1467.

10.1021/la061150b CCC: $37.00
Published on Web 12/09/2006

Cyt. *c* immobilized on Au nanoparticles was retained unlike the free one which gets denatured under drastic conditions of aeorogel formation.[20] Enzymes immobilized on a nanoparticle surface are capable of performing reactions in organic solvents.[21]

Nanoparticles themselves are used for biological applications. Some of the recent examples, although not exhaustive, are listed below. The near-infrared absorbing metal nanoshells and metal nanocages were used in cancer hyperthermia[22] and as targeted contrast agents for diagnostic imaging modalities such as optical coherence tomography.[23] In vivo luminescence imaging of single gold nanorods in mouse ear blood vessels demonstrated a better methodology compared to the same with cytotoxic semiconductor nanocrystals.[24] The oral and transmucosal insulin delivery was carried out with insulin immobilized on aspartate capped gold nanoparticles.[25] In this report we discuss the azide ion binding chemistry of Mb and Hb adsorbed on gold nanoparticles, gold nanorods, and silver nanoparticles. Mb and Hb are oxygen carriers[26] in muscle cells and red blood cells, respectively. We note that Hb immobilized on polyisobutylcyanoacrylate nanoparticles was used as artificial oxygen carriers.[27] Hb capped on clay nanoparticles were used as electrocatalysts.[28] The ligand binding chemistry of Fe(III) containing prosthetic heme *b* group itself was studied to understand the biological activity of oxygen carrying proteins, Mb and Hb.[29,30,31]

In the present study, we used the metabolic inhibitor azide ion as a ligand for heme *b* complex formation studies, due to its intense bands in the Fourier-transform infrared (FTIR) spectra and high solubility in the aqueous medium.[32] Azide binding to heme has been studied to understand conformational changes of Mb and Hb.[29] The present study is part of an ongoing research program on bare metal nanoparticles and core−shell nanoparticles with mercaptans,[33] antibiotics,[34] hemoproteins,[35] and fatty acids.[36,37]

Experimental Section

Materials. Mb (bovine heart muscle) was purchased from Fluka. Hb (bovine) was purchased from Himedia Laboratories, India. Tetrachloroauric acid trihydrate ($HAuCl_4 \cdot 3H_2O$), silver nitrate ($AgNO_3$), cetyl trimethyl ammonium bromide (CTAB), sodium citrate, ascorbic acid, and sodium azide (NaN_3) were purchased from CDH, India. All chemicals were used as such without further purification. Triply distilled deionized water was used for all the experiments. Potassium bromide (spectroscopic grade) used for infrared studies, was purchased from Merck. Sinapinic acid was used as the matrix for MALDI-TOF MS.

Synthesis of Nanoparticle−Hemoprotein Bioconjugates (M@X). Citrate capped Au (and Ag) nanoparticles and Au nanorods were prepared by the methods reported by Turkevich et al.[38] and Sau and Murphy,[39] respectively. The Au (15 nm), Ag (60 nm) nanoparticles, and Au nanorods (aspect ratio: 3.44, diameter: 11 nm) will be referred to below as Au, Ag, and AuNR, respectively. The Au or Ag bioconjugates of Mb or Hb were prepared following a similar procedure as reported before.[35] The AuNR bioconjugates with Mb were synthesized by immobilization of the protein on AuNR, after removing the excess CTAB used for its synthesis. A total of 200 μL of the aqueous solution of purified AuNR was mixed well with 1000 μL of 0.36 mg/mL Mb in aqueous phosphate buffered saline (PBS) at pH 7.2 by means of a vertex. The dispersion was kept at room temperature for 48 h and centrifuged at 8000 rpm. The residue was washed three times with PBS to remove unadsorbed Mb, and the obtained AuNR myoglobin bioconjugate (AuNR@Mb) was dispersed in 200 μL of PBS. Due to the similarity in the chemistry of Mb and Hb evident from nanoparticle studies, only AuNR@Mb bioconjugate was investigated.

Binding of Azide Ion (N_3^-) with Nanoparticle−Hemoprotein Bioconjugates (M@X). The azide binding with Mb and Hb bioconjugates was carried out in the same way, which was adopted in the case of Cyt. *c* bioconjugates.[35] The control experiment of the azide binding to free Mb and Hb at room temperature was performed in the same fashion as reported in the case of free Cyt. *c*.[35]

Instrumentation. UV−visible spectra were measured using a Perkin-Elmer Lambda 25 spectrometer. Transmission electron microscopy (TEM) was performed using a JEOL transmission electron microscope operating at 300 keV. The samples for TEM were prepared by dropping the dispersion on copper grid supported amorphous carbon films. For recording the infrared spectra, vacuum-dried samples were made in the form of 1% (by weight) KBr pellets and the spectra were measured with a Perkin-Elmer Spectrum One FTIR spectrometer. Raman spectra were measured using a Confocal Raman spectrometer CRM 200 of Witec. Mass spectrometric studies were conducted using a Voyager DE PRO Biospectrometry Workstation of Applied Biosystems MALDI-TOF MS. A pulsed nitrogen laser of 337 nm was used (maximum firing rate: 20 Hz, maximum pulse energy: 300 μJ) for MALDI-TOF MS studies. Mass spectra were collected in positive and negative ion modes and were averaged for 100 shots.

Results and Discussion

In contrast to the previous reports[14,15] which investigated surface enhanced Raman spectroscopy and the single molecule spectroscopy of Mb and Hb on metal nanoparticles, in this work we focused on the chemistry of the prosthetic heme *b* unit of the hemoproteins immobilized on metal nanoparticles and nanorods. As binding of Mb and Hb on nanoparticles has been reported before,[14,15] we present only the essential and newer aspects here.

In the UV−visible spectra of the bioconjugates Au@Mb and Au@Hb, the traces (I) show the Soret and surface plasmon resonance (SPR) features (Figure 1). The Soret features of Mb and Hb are observed at 408 and 407 nm, respectively, and were observed after adsorption on the Au nanoparticle surface. This is due to the adsorption of Mb and Hb on Au nanoparticle surface

(19) Wallace, J. M.; Stroud, R. M.; Pietron, J. J.; Long, J. W.; Rolison, D. R. *J. Non-Cryst. Solids* **2004**, *350*, 31−38.
(20) Wallace, J. M.; Dening, B. M.; Eden, K. B.; Stoud, R. M.; Long, J. W.; Rolison, D. R. *Langmuir* **2004**, *20*, 9276−9281.
(21) Phadthare, S.; Vinod, V. P.; Mukhopadhyay, K.; Kumar, A.; Rao, M.; Chaudhari, R. V.; Sastry, M. *Biotechnol. Bioeng.* **2004**, *85*, 629−637.
(22) Hirsch, L. R.; Stafford, R. J.; Bankson, J. A.; Sershen, S. R.; Rivera, B.; Price, R. E.; Hazle, J. D.; Halas, N. J.; West, J. L. *Proc. Natl. Acad. Sci. U.S.A.* **2003**, *100*, 13549−13554.
(23) Chen, J.; Saeki, F.; Wiley: B. J.; Cang, H.; Cobb, M. J.; Li, Z.-Y.; Au, L.; Zhang, H.; Kimmey, M. B.; Li, X.; Xia, Y. *Nano Lett.* **2005**, *5*, 473−477.
(24) Wang, H.; Huff, T. B.; Zweifel, D. A.; He, W.; Low, P. S.; Wei, A.; Cheng, J. X. *Proc. Natl. Acad. Sci. U.S.A.* **2005**, *102*, 15752−15756.
(25) Joshi, H. M.; Bhumkar, D. R.; Joshi, K.; Pokharkar, V.; Sastry, M. *Langmuir* **2006**, *22*, 300−305.
(26) Bormett, R. W.; Asher, S. A.; Larkin, P. J.; Gustafson, W. G.; Ragunathan, N.; Freedman,: T. B.; Nafie, L. A.; Balasubramanian, S.; Boxer, S. G.; Yu, N. T.; Gersonde, K.; Noble, R. W.; Springer, B. A.; Sligar, S. G. *J. Am. Chem. Soc.* **1992**, *114*, 6864−6867.
(27) Chauvierre, C.; Marden, M. C.; Vauthier, C.; Labarre, D.; Couvreur, P.; Leclerc, L. *Biomaterials* **2004**, *25*, 3081−3086.
(28) Liu, Y.; Liu, H.; Hu, N. *Biophys. Chem.* **2005**, *117*, 27−37.
(29) Hille, R.; Olson, J. S.; Palmer, G. *J. Biol. Chem.* **1979**, *254*, 12110−12120.
(30) Maurus, R.; Bogumil, R.; Nguyen, N. T.; Mauk, A. G.; Brayer, G. *Biochem. J.* **1998**, *332*, 67−74.
(31) Lim, M.; Hamm, P.; Hochstrasser, R. M. *Proc. Natl. Acad. Sci. U.S.A.* **1998**, *95*, 15315−15320.
(32) Yoshikawa, S.; Caughey, W. S. *J. Biol. Chem.* **1992**, *267*, 9757−9766.
(33) Sandhyarani, N.; Pradeep, T. *Int. Rev. Phys. Chem.* **2003**, *22*, 221−262.
(34) Tom, R. T.; Suryanarayanan, V.; Reddy, P. G.; Baskaran, S.; Pradeep, T. *Langmuir* **2004**, *20*, 1909−1914.
(35) Tom, R. T.; Pradeep, T. *Langmuir* **2005**, *21*, 11896−11902.
(36) Tom, R. T.; Nair, A. S.; Singh, N.; Aslam, M.; Nagendra, C. L.; Philip, R.; Vijayamohanan, K.; Pradeep, T. *Langmuir* **2003**, *19*, 3439−3445.
(37) Nair, A. S.; Pradeep, T.; MacLaren, I. *J. Mater. Chem.* **2004**, *14*, 857−862.
(38) Turkevich, J.; Stevenson, P. C.; Hillier, J. *Discuss. Faraday Soc.* **1951**, *11*, 55−75.
(39) Sau, T. K.; Murphy, C. J. *Langmuir* **2004**, *20*, 6414−6420.

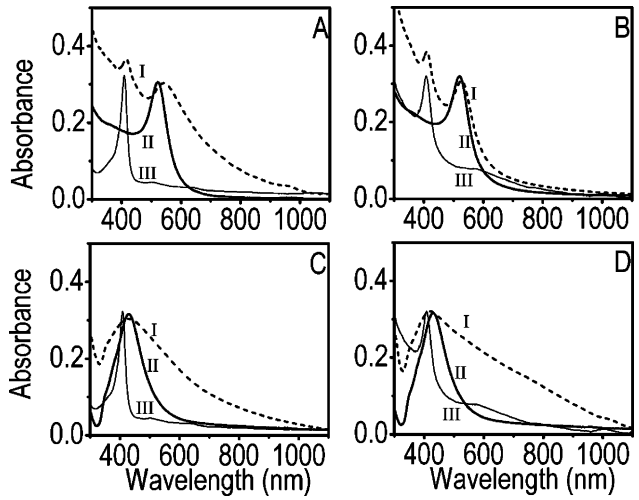

Figure 1. Absorption spectra of the M@X nanoparticle system. The panels A, B, C, and D correspond to the samples Au@Mb, Au@Hb, Ag@Mb, and Ag@Hb, respectively. Traces I, II, and III of all figures correspond to 0.2 mg/mL M@X, 0.1 mg/mL M@Cit, and 0.1 mg/mL X, respectively.

in a multilayer fashion.[40] The SPR band of Au nanoparticle was red-shifted from 520 to 543 nm and 527 nm after the capping with Mb (Figure 1A) and Hb (Figure 1B), respectively. Cyt. *c* capping on Au nanoparticles was shown to give a shift of the SPR band to 590 nm. This variation in the SPR band of gold nanoparticles capped with Cyt. *c*, Mb, and Hb is due to the difference in the tendency of the proteins for forming multilayer assemblies.[40] The UV visible features of Ag@Mb (Figure 1C) and Ag@Hb (Figure 1D) showed aggregated features, similar to that observed earlier in the case of Ag@Cyt. *c*.[35] The Soret feature of free Mb and Hb shown in the traces (III) is merged with the aggregated SPR band in these cases, similar to that of Ag@Cyt. *c*.[35] The intensity of the Soret band of X (Mb or Hb) which remained in the mother liquor after complete removal of M@X by centrifugation (starting from a known concentration) was used for calculating the number of molecules per nanoparticle. These calculations were done in a way similar to that reported earlier in the case of Cyt. *c*.[35] The number of molecules per nanoparticle is 587, 283, 4834, and 2858 for Au@Mb, Au@Hb, Ag@Mb, and Ag@Hb, respectively. The values reported for Au@Cyt. *c* and Ag@Cyt. *c* were 700 and 6127, respectively,[35] indicating a thicker multilayer for Cyt. *c*. leading to a larger shift in the SPR band. The experimental observation is consistent with a calculation of multilayer assembly (Supporting Information 1).

The TEM images of Au@Hb (Figure 2A) and Au@Mb (Figure 2D) showed uniform sized particles (15 nm) with lower extent of aggregation, similar to Au@Cyt. *c*.[35] From the TEM and absorption spectrum, it is clear that multilayer adsorption of hemoproteins on the surface of spherical Au nanoparticles prevents the contact of neighboring nanoparticles, thereby blocking the nanoparticle aggregation. High-resolution images of Au@Hb (Figure 2B,C) showed multiple lattice fringes on a single particle, indicating the polycrystalline nature of the metal core. The TEM images of Ag@Mb, (Figure 2E) and Ag@Hb (Figure 2F) showed particles with different sizes and shapes. Unlike Au nanoparticles, Ag nanoparticles formed by the citrate reduction are polydisperse and contain spherical particles, rods and several other shapes[41] and are prone to aggregation.[35]

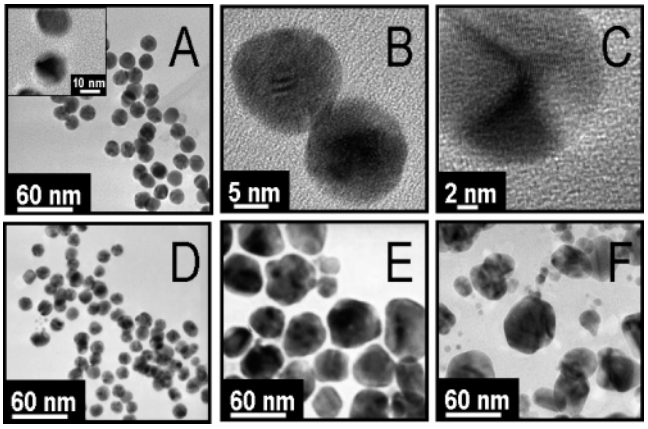

Figure 2. Transmission electron micrographs of Hb and Mb capped Au nanoparticles, showing uniform sized particles (A and D, respectively). The core−shell structure is shown in the under focused image of Au@Hb (inset of panel A). Panels B and C represent the lattice resolved images of Au@Hb, which show the polycrystalline nature of the gold core. Panels E and F represent the transmission electron micrograph of Mb and Hb capped Ag nanoparticles, respectively, which show polydispersed particles, typical of citrate synthesis.

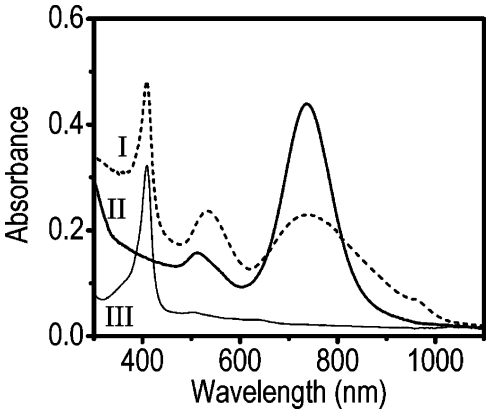

Figure 3. UV−visible spectra of AuNR@Mb (I), pure AuNR (II), and Mb(III) 0.1 mg/mL in PBS.

In Figure 3, traces II and I correspond to the UV−visible absorption spectra of the purified AuNR solution in water and AuNR@Mb in aqueous PBS, respectively. Pure Mb shows the Soret band of Mb at 408 nm (trace III). The nanorods show two peaks at 736 and 510 nm corresponding to the longitudinal and transverse plasmons,[39] respectively, suggesting an aspect ratio as 3.44, which is also evident from the HRTEM results. After binding to Mb, the peaks corresponding to the longitudinal and transverse plasmons were shifted to 740 and 534 nm, respectively. Dampening and broadening of the longitudinal plasmon is due to aggregation of nanorods after the binding of Mb.[42] The fast exchange of CTAB bilayer on AuNR surface by Mb resulted in the aggregation of nanorods by cross-linking them in a nondirectional fashion.[43−44] The Soret band of Mb remained unaffected after adsorption on the Au nanorods. The shift as well as broadening of the SPR bands after bioconjugation is attributed to the formation of aggregates. The HRTEM images Figure 4A,B and Figure 4C,D represent pure nanorods and AuNR@Mb

(40) Jiang, X.; Jiang, J.; Jin, Y.; Wang, E.; Dong, S. *Biomacromolecules* **2005**, *6*, 46−53.

(41) Bright, R. M.; Musick, M. D.; Natan, M. J. *Langmuir* **1998**, *14*, 5695−5701.

(42) Joseph, S. T. S.; Ipe, B. I.; Pramod, P.; Thomas, K. G. *J. Phys. Chem. B* **2006**, *110*, 150−157.

(43) Thomas, K. G.; Barazzouk, S.; Ipe, B. I.; Joseph, S. T. S.; Kamat, P. V. *J. Phys. Chem. B* **2004**, *108*, 13066−13068.

(44) Jain, P. K.; Eustis, S.; El-Sayed, M. A. *J. Phys. Chem. B* **2006**, *110*, 18243−18253

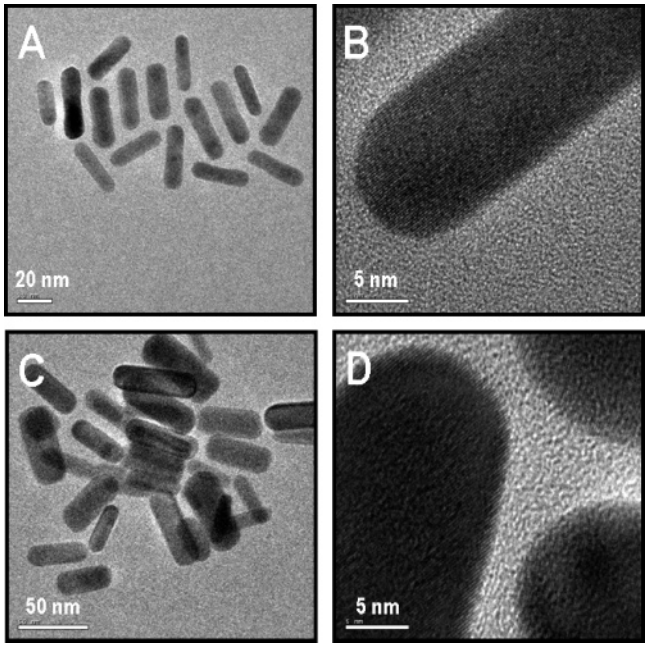

Figure 4. HRTEM images of neat AuNR (A, B) and AuNR@Mb (C, D). Panels B and D are lattice resolved.

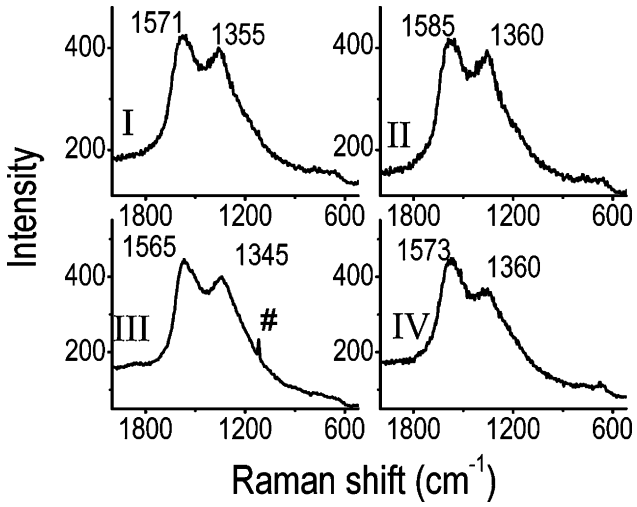

Figure 5. Raman spectra recorded using 514.5 nm laser excitation through a confocal (60 X) objective. The traces I, II, III, and IV correspond to Mb, Ag@Mb, Hb, and Ag@Hb, respectively. The peak around 1100 cm^{-1} (marked with #) in trace III corresponds to the Raman feature of the cover glass slip used for the experiment.

bioconjugates, respectively. The bioconjugate sample showed aggregated structures, which agrees with the broadening of the SPR bands. Panels B and C of Figure 4 show lattice resolved images which do not indicate any change in morphology or structure after protein binding.Both Mb and Hb have Raman active heme *b* as the prosthetic group. In our earlier work, we observed well-defined Raman features for Hemin capped Ag nanoparticles. Both silver hemoprotein bioconjugates, Ag@Mb and Ag@Hb, showed intense Raman bands. The Raman spectrum of Mb (I) shows major bands at 1571 and 1355 cm^{-1} which correspond to the merged asymmetric C−C stretching ($\nu_{10}(C_\alpha-C_m)_{asym}$, $\nu_2(C_\beta-C_\beta)_{asym}$) and symmetric pyrrole-half-ring stretching bands (ν_4(Pyr half-ring)$_{sym}$), respectively.[15,45] After adsorption on Ag nanoparticles (II), the Raman bands characteristic of the

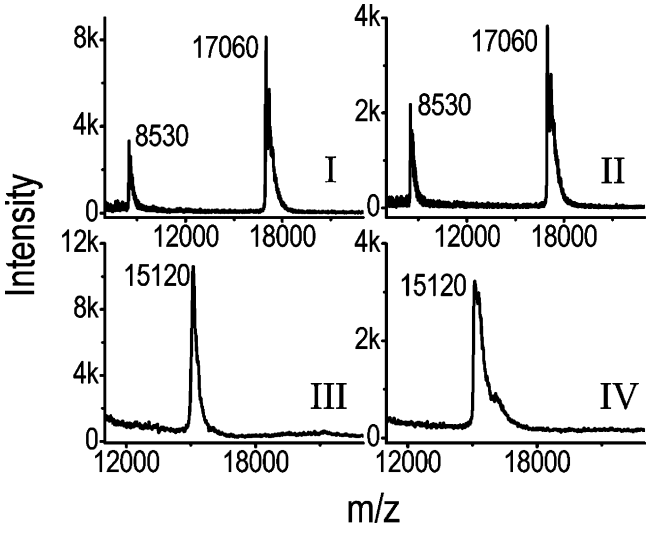

Figure 6. MALDI-TOF mass spectra of the samples measured with 337 nm N_2 laser using sinapinic acid matrix. The traces I, II, III, and IV correspond to Mb, Au@Mb, Hb, and Au@Hb, respectively.

prosthetic heme *b* unit of Mb, the merged ν_{10}/ν_2 and ν_4 were shifted from 1571 to 1585 cm^{-1} and 1355 to 1360 cm^{-1}, respectively. Raman spectrum of AuNR@Mb has more resolved features for $\nu_{10}(C_\alpha-C_m)_{asym}$, $\nu_2(C_\beta-C_\beta)_{asym}$, and ν_4(Pyr half-ring)$_{sym}$ compared to the spectrum of Au@Mb (Supporting Information 2). Thus, it is clear that the spectra of X and M@X are inherently broad at this excitation. A better resolved spectrum of Mb has been reported by Feng and Tachikawa,[46] and the difference between the two data is likely to be due to the different source of Mb used (horse skeletal muscle for the former). It appears that improved spectral quality for AuNR@Mb is due to the specific enhancement due to AuNRs.[47]

The samples Mb and Au@Mb showed molecular ion peak at *m*/*z* 17060 and a doubly charged molecular ion at *m*/*z* 8530 in the positive ion mode[16] in the MALDI MS (Figure 6). Similarly MALDI-TOF MS analysis of Hb and Au@Hb showed a characteristic peak at *m*/*z* 15120, which corresponds to the monomer unit of the tetrameric Hb molecule.[48] The nanorod bioconjugate, AuNR@Mb, showed the molecular ion peak at *m*/*z* 17060 and the doubly charged molecular ion at *m*/*z* 8530 in MALDI-TOF MS analysis (Supporting Information 3). The MALDI-TOF MS analysis confirmed the capping of hemoproteins on the nanoparticles and the nanorod. The usefulness of mass spectrometry in characterizing bioconjugates was shown in our previous report as well.[35]

Cyt. *c* immobilized on gold and silver nanoparticles showed absence of reactivity with azide ions at room temperature.[35] There was no shift for the Soret band of Cyt. *c* in the presence of azide ion without thermal activation. Unlike in the oxygen carriers Mb and Hb, the prosthetic heme group is less accessible to reactants in the case of Cyt. *c* due to the conformational rigidity of the latter. The Soret band in Au@Hb was shifted from 407 to 415 nm due to complexation with azide. The shift was from 527 to 533 nm for the SPR band. Part of the shift of the SPR band could be due to azide ion binding on the nanoparticle directly (Figure 7A). The increase in the background intensity indicates the aggregation of the sample after complexation. Control experiments were carried out with free Mb and Hb in presence of azide

(45) Wood, B. R.; Langford, S. J.; Cooke, B. M.; Lim, J.; Glenister, F. K.; Duriska, M.; Unthank, J. K.; McNaughton, D. *J. Am. Chem. Soc.* **2004**, *126*, 9233−9239.

(46) Feng, M.; Tachikawa, H. *J. Am. Chem. Soc.* **2001**, *123*, 3013−3020.

(47) Orendorff, C. J.; Gearheart, L.; Jana, N. R.; Murphy, C. J. *Phys. Chem. Chem. Phys.* **2006**, *8*, 165−170.

(48) Kiernan, U. A.; Black, J. A.; Williams, P.; Nelson, R. W. *Clin. Chem.* **2002**, *48*, 947−949.

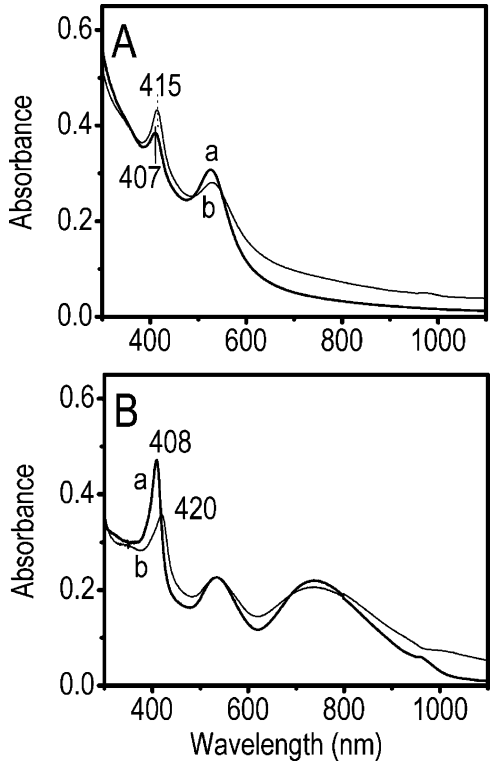

Figure 7. UV−visible spectrum of the samples in aqueous phosphate buffered saline (PBS). (A) Au@Hb (thick trace, a) and Au@Hb-N_3 (thin trace, b); (B) AuNR@Mb (thick trace, a) and AuNR@Mb-N_3 (thin trace, b).

ion at room temperature. The Soret band was shifted from 407 to 417 nm for Hb due to complexation (Supporting Information 4). The UV/vis spectra show that the microenvironment of the prosthetic heme group of Mb and Hb is more accessible to azide ion compared to the same in Cyt. *c*. Similar kinds of features are noticed in the case of bioconjugates of gold nanorods. Red shift was observed from 408 to 420 nm for the Soret band, from 742 to 752 nm for the longitudinal plasmon band, and from 534 to 538 nm for the transverse plasmon band, after the complexation of AuNR@Mb with azide (Figure 7B). The Soret band was shifted from 408 to 422 nm for neat Mb, in the control experiment (Supporting Information 4).

In agreement with the UV/vis data, the TEM images show that particles are well separated and show no sign of aggregation (Figure 8A). The polycrystalline gold core of Au@Hb-N_3 is observed in high-resolution image (Figure 8B) similar to Au@Hb (Figure 2B,C). From the UV−visible and TEM studies, it is clear that Au@Hb bioconjugate is stable during the reaction with azide.

Azide binding was investigated using FTIR (Supporting Information 5). For comparison of the features, spectra of azide bound nanoparticles were also measured. Asymmetric stretching, ν_{as} (N_3) of the free azide was observed at 2036 cm^{-1} in the FTIR spectrum.[49] This feature, observed in the traces marked (I) for all the figures (A−D), is due to the presence of azide ion bound directly to the metal surface of the nanoparticle through electrostatic interactions. This band, marked with a line, is the dominant feature in traces II, which correspond to M@N_3.The

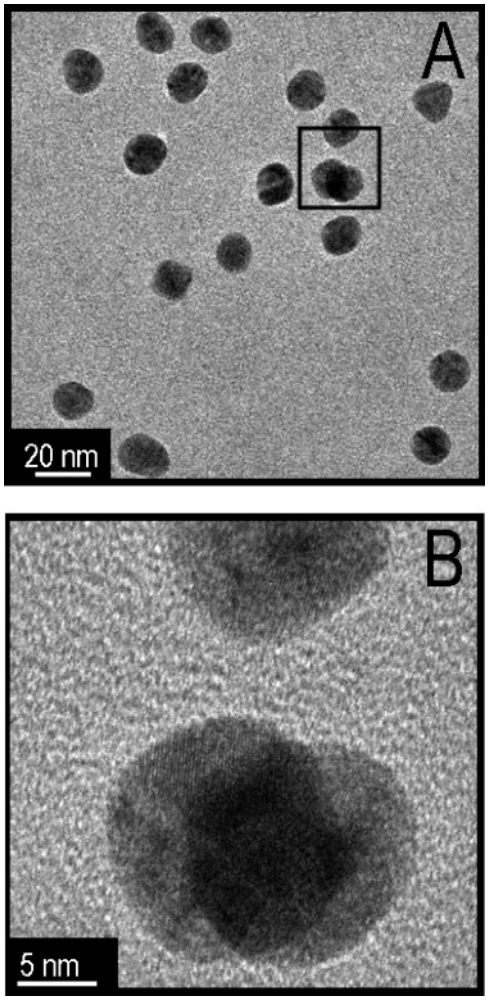

Figure 8. TEM images of Au@Hb-N_3. Well-separated particles are observed in image A. The image B corresponds to an enlarged view of the marked portion in image A, showing the lattices of the gold nanoparticles.

broad peak observed in traces I near 2050 cm^{-1} is due to the azide ion bound to the Fe(III) center of the prosthetic heme.[50−51] The traces III correspond to the bioconjugates (M@X), which do not show any characteristic feature in the above-mentioned region. The FTIR analysis of AuNR@Mb-N_3 also showed the asymmetric stretching of the Fe(III) bound azide ion at 2050 cm^{-1} (Supporting Information 6). The similarity in the reactivity of Mb, Au@Mb, and AuNR@Mb with azide ion indicates the retention of the molecular structure of the protein after immobilization on both Au nanoparticles and Au nanorods.

Summary and Conclusions

The immobilization of hemoproteins on surfaces of Au and Ag nanoparticles and Au nanorods has been investigated. The bioconjugates formed were characterized by UV−visible spectroscopy and HRTEM. The bioconjugates of Au have better dispersability and show less aggregation in comparison to the Ag analogues. The bioconjugates showed hardened Raman features of the prosthetic heme moiety, a signature of surface confinement. The molecular ion signature of hemoproteins obtained in the MALDI-TOF MS analysis confirmed the capping of hemoproteins on the nanoparticles and nanorods. The chemical reactivity of the heme was probed using the azide ion. A red shift in the Soret band was observed both in the case of hemoproteins and bioconjugates after the azide binding to the heme. The azide complexation was further confirmed by FTIR spectroscopy. The

(49) Miksa, D.; Brill, T. B. *J. Phys. Chem. A* **2003**, *107*, 3764−3768.
(50) Bormett, R. W.; Asher, S. A.; Larkin, P. J.; Gustafson, W. G.; Ragunathan, N.; Freedman,: T. B.; Nafie, L. A.; Balasubramanian, S.; Boxer, S. G.; Yu, N. T.; Gersonde, K.; Noble, R. W.; Springer, B. A.; Sligar, S. G. *J. Am. Chem. Soc.* **1992**, *114*, 6864−6867.
(51) Neya, S.; Tsubaki, M.; Hori, H.; Yonetani, T.; Funasaki, N. *Inorg. Chem.* **2001**, *40*, 1220−1225.

TEM and UV−visible spectroscopy studies confirm that there were no morphology changes during azide binding chemistry. This work demonstrates the fact that the structure and reactivity of Hb and Mb are unaffected upon binding to noble metal nanoparticles, which suggests the use of nanoparticle−metalloprotein hybrid systems in biochemical reactions.

Acknowledgment. We thank the Department of Science and Technology, Government of India, for constantly supporting our research program on nanomaterials. R.T.T. thanks the Council of Scientific and Industrial Research (CSIR) for a senior research fellowship.

Supporting Information Available: Calculation of surface coverage, Raman spectra of Mb and AuNR@Mb, MALDI-TOF mass spectra of Mb and AuNR@Mb, UV−visible spectra of free Hb and Mb before and after complexation with azide, and FTIR spectra of azide complexes of Au@Mb, Ag@Mb, Au@Hb, Ag@Hb, and AuNR@Mb. This material is available free of charge via the Internet at http://pubs.acs.org.

LA061150B